SET-MEMBERSHIP IDENTIFICATION OF WIENER MODELS WITH NON-INVERTIBLE NONLINEARITY

Vito Cerone [*,1] **Diego Regruto** [*]

[*] *Dipartimento di Automatica e Informatica, Politecnico di Torino, Corso Duca degli Abruzzi 24, 10129 Torino, Italy, e-mail: vito.cerone@polito.it, diego.regruto@polito.it*

Abstract: In this paper the identification of SISO Wiener models in presence of bounded output noise is considered. A three stage procedure based on the inner signal estimation, outlined in a previous contribution, has been proposed. Results and algorithms for the computation of inner-signal bounds through the design of a suitable input sequence have been provided for the case of polynomial without invertibility assumptions. A simulated example, showing the effectiveness of the proposed approach, has been presented.

Keywords: Identification, nonlinear models, parameter estimation, uncertainty, bounded noise.

1. INTRODUCTION

In this paper we will focus on a particular class of nonlinear systems, commonly referred to as Wiener models (see Figure 1) which consists of a linear dynamic system followed by static nonlinear block $\mathcal{N}$. The identification of such a model is carried out on the basis of the sequences u_t and y_t, while the inner signal x_t, i.e. the output of the linear block, is not assumed to be available. Despite its simplicity, such model has been successfully used in many engineering fields, thanks to its ability to embed process structure knowledge like, e.g., the presence of nonlinearity in the measurement equipment. The identification of Wiener models has attracted the attention of many authors exploiting a number of different techniques (see, e.g., Billings, 1980; Bai, 2003; Wigren, 1993; Crama and Schoukens, 2001; Greblicki, 1992). The main difficulty in the identification of nonlinear block-oriented systems is that the internal signal is not available for measurement. Most of the contributions assume invertibility of the nonlinearity; as a matter of fact under such an assumption the inner signal can be recovered from the output measurements through inversion of the previously estimated nonlinearity. However, many output nonlinearities encountered in real world problems are non-invertible, thus the invertibility assumption appears to be quite restrictive.

In all the papers mentioned above, the authors assume that the measurement error η_t is statistically described. This paper deals with the identification of Wiener models with non-invertible nonlinearity when the measurement errors are assumed to be *unknown but bounded* (see, e.g., Milanese *et al.*, 1996). The key step in the proposed procedure is the inner signal estimation since the nonlinearity is assumed to be non-invertible, which means that, given the measured output y_t, the inner signal x_t cannot be evaluated uniquely even in the case of exactly known polynomial and noise free measurements. Some guidelines on how to deal with this problem through the design of a suitable identification experiment have been provided in (Cerone *et al.*, 2003). In this paper algorithms for the solution of such a problem are provided together with a simulated example showing the effectiveness of the proposed approach.

[1] Corresponding author

2. SET MEMBERSHIP IDENTIFICATION OF WIENER SYSTEMS

Consider the SISO discrete-time Wiener model shown in Figure 1, where the linear dynamic block, which is modeled by a stable discrete-time system with non-zero steady-state gain, maps the input signal u_t into the unmeasurable inner variable x_t according to

$$x_t = \frac{B(q^{-1})}{A(q^{-1})} u_t = G(q^{-1}) u_t, \qquad (1)$$

where $A(\cdot)$ and $B(\cdot)$ are polynomials in the backward shift operator q^{-1}, ($q^{-1} w_t = w_{t-1}$),

$$A(q^{-1}) = 1 + a_1 q^{-1} + \ldots + a_{na} q^{-na}, \qquad (2)$$

$$B(q^{-1}) = b_0 + b_1 q^{-1} + \ldots + b_{nb} q^{-nb}. \qquad (3)$$

and $A(\cdot)$ is assumed to be stable. The nonlinear block transforms x_t into the noise-free output w_t through the following polynomial function $\mathcal{N}(x_t, \gamma)$

$$w_t = \mathcal{N}(x_t, \gamma) = \sum_{k=1}^{n} \gamma_k x_t^k, \quad t = 1, \ldots, N; \qquad (4)$$

whose order n is taken to be finite and a-priori known; N is the length of the input sequence. Let y_t be the noise-corrupted measurements of w_t

$$y_t = w_t + \eta_t. \qquad (5)$$

Measurements uncertainty is known to range within given bounds $\Delta\eta_t$, i.e.,

$$\mid \eta_t \mid \leq \Delta\eta_t. \qquad (6)$$

Unknown parameter vectors $\gamma \in R^n$ and $\theta \in R^p$ are defined, respectively, as $\gamma^T = [\gamma_1 \quad \gamma_2 \quad \ldots \gamma_n]$, $\theta^T = [a_1 \quad \ldots \quad a_{na} \quad b_0 \quad b_1 \quad \ldots b_{nb}]$. Since the parameterization of the structure of Figure 1 is not unique we assume without loss of generality, that the steady-state gain of the linear part be one, that is $g = \sum_{j=0}^{nb} b_j \Big/ (1 + \sum_{i=1}^{na} a_i) = 1$. Preliminary results on set-membership identification of Wiener models described by equations (1) – (6) have been provided in (Cerone *et al.*, 2003). The three-stage procedure for deriving bounds on parameters γ and θ outlined in that paper can be summarized as follows. First, exploiting M steady-state input-output data, one gets the feasible parameter set $\mathcal{D}_\gamma$ of the nonlinear block parameters, which is a convex polytope; then the central estimate ${\gamma_j}^c = \left(\gamma_j^{min} + \gamma_j^{max}\right) / 2$ and the parameter uncertainty interval $[\gamma_j^{min}, \gamma_j^{max}]$ of each parameter γ_j are computed solving the following two linear programming problems:

$$\gamma_j^{min} = \min_{\gamma \in \mathcal{D}_\gamma} \gamma_j, \quad \gamma_j^{max} = \max_{\gamma \in \mathcal{D}_\gamma} \gamma_j, \qquad (7)$$

$${\gamma_j}^c = \frac{\gamma_j^{min} + \gamma_j^{max}}{2}. \qquad (8)$$

Further, given the estimated uncertain nonlinearity $\mathcal{N}(x_t, \gamma)$ and the output measurements collected exciting the system with an input dynamic signal, bounds on the inner signal x_t are computed. Finally, such bounds, together with the input dynamic sequence, are used for bounding the parameters of the linear block solving a suitable output error problem.

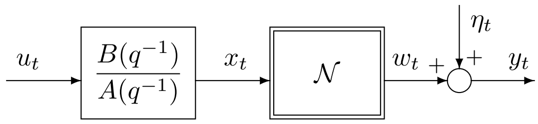

Fig. 1. Single-input single-output Wiener model.

3. EXPERIMENT DESIGN AND ESTIMATION OF THE INNER SIGNAL

In the case of uncertain polynomial the following family of polynomials can be defined

$$\Pi_t = \{p_t(x_t, w_t, \gamma) : w_t \in R, \ \gamma \in \mathcal{D}_\gamma\} \qquad (9)$$

where

$$p_t(x_t, w_t, \gamma) = w_t - \sum_{k=1}^{n} \gamma_k x_t^k. \qquad (10)$$

It is assumed that all polynomials in Π_t have degree equal to n, that is, $\gamma_n \neq 0 \ \forall \gamma \in \mathcal{D}_\gamma$. In order to evaluate the inner signal x_t one has to find the real roots of the uncertain polynomial (9).
Now, let us introduce the following definitions of *Output Invertibility Interval* and *Feasible Inner-signal Interval*.

Definition 1. The set $W \subset R$ is an **Output Invertibility Interval** for the uncertain polynomial $\mathcal{N}(x_t, \gamma)$ of order n, if for $w_t \in W$ each polynomial $p_t(x_t, w_t, \gamma) \in \Pi_t$ shows either only one real root when n is odd or two real roots when n is even.

Definition 2. The set $X \subset R$ is a **Feasible Inner-signal Interval** for the Wiener system described by equations (1), (2), (3) and (4) if the set of output values $\mathcal{O} = \{w_t \in R : w_t = \mathcal{N}(x_t, \gamma),$ for some $\gamma \in \mathcal{D}_\gamma, \ x_t \in X\}$ is an **Output Invertibility Interval**.

The key idea exploited in this paper is to design an input sequence $\{u_t\}$ which will force the unmeasurable inner sequence $\{x_t\}$ to belong to a prescribed *Feasible Inner-signal Interval* X. In such a way the corresponding output sequence $\{w_t\}$ will belong to an *Output Invertibility Interval* of the polynomial $\mathcal{N}(x, \gamma)$.
The following three propositions provide a characterization of the Output Invertibility Intervals and the Feasible Inner-signal Intervals.

***Proposition** 1.* The uncertain polynomial $\mathcal{N}(x_t, \gamma)$ with $\gamma \in \mathcal{D}_\gamma$, exhibits the following two Output Invertibility Intervals when n is odd:

$$\overline{W} =]\overline{w}, +\infty[\ \text{ and } \ \underline{W} =]-\infty, \underline{w}[\qquad (11)$$

where

$$\overline{w} = \max_{x_t \in \Upsilon_t} \max_{\gamma \in \mathcal{D}_\gamma} \sum_{k=1}^{n} \gamma_k x_t^k \tag{12}$$

$$\underline{w} = \min_{x_t \in \Upsilon_t} \min_{\gamma \in \mathcal{D}_\gamma} \sum_{k=1}^{n} \gamma_k x_t^k \tag{13}$$

$$\Upsilon_t = \left\{ x_t \in R \colon \frac{d}{dx_t} \sum_{k=1}^{n} \gamma_k x_t^k = 0, \text{for some } \gamma \in \mathcal{D}_\gamma \right\} \tag{14}$$

Proof: see (Cerone and Regruto, 2004).

***Proposition** 2.* The uncertain polynomial $\mathcal{N}(x_t, \gamma)$ with $\gamma \in \mathcal{D}_\gamma$, exhibits the following Output Invertibility Intervals when n is even:

$$\overline{W} =]\overline{w}, +\infty] \quad \text{for} \quad \gamma_n > 0 \tag{15}$$

and

$$\underline{W} = [-\infty, \underline{w}[\quad \text{for} \quad \gamma_n < 0 \tag{16}$$

where

$$\overline{w} = \max_{x_t \in \Upsilon_t} \max_{\gamma \in \mathcal{D}_\gamma} \sum_{k=1}^{n} \gamma_k x_t^k \tag{17}$$

$$\underline{w} = \min_{x_t \in \Upsilon_t} \min_{\gamma \in \mathcal{D}_\gamma} \sum_{k=1}^{n} \gamma_k x_t^k \tag{18}$$

$$\Upsilon_t = \left\{ x_t \in R \colon \frac{d}{dx_t} \sum_{k=1}^{n} \gamma_k x_t^k = 0, \text{for some } \gamma \in \mathcal{D}_\gamma \right\} \tag{19}$$

Proof: see (Cerone and Regruto, 2004).

***Proposition** 3.* The Wiener system described by equations (1), (2), (3) and (4), with uncertain output polynomial $\mathcal{N}(x_t, \gamma)$, exhibits the following Feasible Inner-signal Intervals:

$$\overline{X} =]\overline{x}, +\infty[\tag{20}$$

and

$$\underline{X} =]-\infty, \ \underline{x}[\tag{21}$$

where

$$\overline{x} = \max \left\{ x_t \in R : \frac{1 + \text{sign}(\gamma_n)}{2} \overline{w} + \frac{1 - \text{sign}(\gamma_n)}{2} \underline{w} - \sum_{k=1}^{n} \gamma_k x_t^k = 0, \text{for some } \gamma \in \mathcal{D}_\gamma \right\} \tag{22}$$

$$\underline{x} = \min \left\{ x_t \in R : \frac{1 + (-1)^n \text{sign}(\gamma_n)}{2} \overline{w} + \frac{1 - (-1)^n \text{sign}(\gamma_n)}{2} \underline{w} - \sum_{k=1}^{n} \gamma_k x_t^k = 0, \text{for some } \gamma \in \mathcal{D}_\gamma \right\} \tag{23}$$

Proof: see (Cerone and Regruto, 2004).

3.1 Input sequence design

In order to drive the inner signal $\{x_t\}$ into the desired interval X, the input signal $\{u_t\}$ should contain a DC component u_{DC} (offset) and a dynamic exciting signal $\{u_{td}\}$ whose amplitudes should be chosen in such a way that $x_t = x_{DC} + x_{td}$ belongs to X $\forall t$. Since the steady-state gain of the linear subsystem is constrained to be one, the amplitudes of the DC components in $u_t = u_{DC} + u_{td}$ and x_t are the same, i.e., $u_{DC} = x_{DC}$. Guidelines for the design of the dynamic exciting signal $\{u_{td}\}$ are provided by the following two propositions straightforwardly derived from the definition of ℓ_∞-norm/ℓ_∞-norm system gain which equals the ℓ_1-norm of h.

***Proposition** 4.* For a given $u_{DC} \geq \overline{x}$, each sample of the sequence $\{x_t\}$ belongs to $\overline{X}$ if:

$$\|\{u_{td}\}\|_\infty \leq \frac{|u_{DC} - \overline{x}|}{h_{up}} \tag{24}$$

where h is the impulse response of the linear block and h_{up} is an upper bound of its ℓ_1 norm; $\|\cdot\|_\infty$ is the ℓ_∞ norm of a sequence.

***Proposition** 5.* For given $u_{DC} \leq \underline{x}$, each sample of the sequence $\{x_t\}$ belongs to $\underline{X}$ if:

$$\|\{u_{td}\}\|_\infty \leq \frac{|u_{DC} - \underline{x}|}{h_{up}} \tag{25}$$

When no a priori information on the ℓ_1-norm of the linear systems is available, the following result can be exploited.

***Proposition** 6.* All the samples of the output sequence $\{w_t\}$ belong to the same Output Invertibility Interval W (either $W = \overline{W}$ or $W = \underline{W}$) if the samples of the corresponding measured output sequence $\{y_t\}$ satisfy the following inequalities:

$$y_t > \overline{y} \ \forall t \ \text{ or } \ y_t < \underline{y} \ \forall t, \ \text{ when } n \text{ is odd} \tag{26}$$

or

$$\text{sign}(\gamma_n)(y_t - \text{sign}(\gamma_n)\Delta\eta_t) > \frac{1 + \text{sign}(\gamma_n)}{2}\overline{y} - \frac{1 - \text{sign}(\gamma_n)}{2}\underline{y}, \ \forall t \ \text{ when } n \text{ is even} \tag{27}$$

where

$$\overline{y} = \overline{w} + \Delta\eta_t, \quad \underline{y} = \underline{w} - \Delta\eta_t$$

Proof: see (Cerone and Regruto, 2004).

Proposition 6 provides sufficient conditions for $\{w_t\}$ to belong either to $\overline{W}$ or to $\underline{W}$. Thus, when no a priori information on the ℓ_1-norm of the linear systems is available, the condition $x_t \in X \ \forall t$ can be indirectly satisfied varying the amplitude of the dynamic sequence $\{u_{td}\}$ by trial and error until the measured output sequence $\{y_t\}$ satisfies either condition (26), when n is odd, or condition (27), when n is even.

3.2 Evaluation of bounds on the unmeasurable inner signal

Given the estimated uncertain polynomial nonlinearity and a sequence of measured outputs $\{y_t\}$, obtained exciting the Wiener system with a suitable input sequence $\{u_t\}$ as described in Section 3.1, in this section it is shown how upper and lower bounds on the samples of the unmeasurable inner signal x_t can be evaluated.

The following proposition provides the bounds for the case $\gamma_n > 0$ and $X = \overline{X}$. The analogous propositions for the other cases are not reported due to lack of space, since they are only slightly variations of this result.

***Proposition** 7.* Given the estimated polynomial nonlinearity $\mathcal{N}(x_t, \gamma)$ with $\gamma \in \mathcal{D}_\gamma$ and $\gamma_n > 0$, an input sequence $\{u_t\}$ which drives the inner unmeasurable signal into a Feasible Inner-signal Interval $\overline{X}$, and the corresponding measured output sequence $\{y_t\}$, each sample x_t of the inner sequence $\{x_t\}$ is bounded as follows:

$$x_t^{min} \leq x_t \leq x_t^{max} \tag{28}$$

where:

$$x_t^{max} = \max\left\{ x_t \in \overline{X} : y_t + \Delta\eta_t - \sum_{k=1}^{n} \gamma_k x_t^k = 0, \right. \\ \left. \text{for some } \gamma \in \mathcal{D}_\gamma \right\} \tag{29}$$

$$x_t^{min} = \max\left\{ \overline{x}, \hat{x}_t^{min} \right\}$$

$$\hat{x}_t^{min} = \min\left\{ x_t \in R : y_t - \Delta\eta_t - \sum_{k=1}^{n} \gamma_k x_t^k = 0, \right. \\ \left. \text{for some } \gamma \in \mathcal{D}_\gamma \right\} \tag{30}$$

Proof: see (Cerone and Regruto, 2004).

4. COMPUTATIONAL ALGORITHMS

In this section the computational aspects of quantities and sets involved in the estimation of the inner signal are analyzed.

Computation of Υ_t — First consider the set defined by equation (14), i.e., the set of real valued x_t for which the uncertain polynomial shows stationary points (relative maxima, relative minima or points of inflexion). The first derivative of the uncertain polynomial is still an uncertain polynomial, namely

$$p_t{}'(x_t, \gamma) = -\frac{d}{dx_t} \sum_{k=1}^{n} \gamma_k x_t^k = -\sum_{k=1}^{n} k\gamma_k x_t^{k-1} \tag{31}$$

which, clearly, shows nonlinear relations in the unknown x_t and the uncertain γ. It is noticed that a given $x_t \in R$ is a real root of the uncertain polynomial (31) if and only if there exists at least one $\gamma \in \mathcal{D}_\gamma$ such that x_t is the solution of the equation $\sum_{k=1}^{n} k\gamma_k x_t^{k-1} = 0$. In order to find the real roots of (31), a one-dimensional gridding on the variable x_t is proposed. For each grid point x_t one must check if there exists a solution to a set of $2M$ linear inequalities (i.e., $\gamma \in \mathcal{D}_\gamma$) and one linear equality (i.e., $\sum_{k=1}^{n} k\gamma_k x_t^{k-1} = 0$) in the unknown $\gamma \in R^n$. If a solution γ exists, then x_t is a real roots of the uncertain polynomial (31). Such a check can be performed solving a linear programming problem.

Computation of $\overline{w}$ and $\underline{w}$ — Next equations (12) and (13) which define two nonlinear programming problems are considered. We note that when x_t is given, problems (12) and (13) simplify to linear programs. Thus, to compute $\overline{w}$ and $\underline{w}$, for each value of $x_t \in \Upsilon_t$, the solution of two linear programming problems with n variables and $2M$ constraints is required. A one-dimensional gridding procedure is used in order to carry out the optimization over a finite number of $x_t \in \Upsilon_t$.

Computation of $\overline{x}$ and $\underline{x}$ — Here, equation (22) and equation (23) are considered. In order to simplify the discussion, only odd order polynomials with $\gamma_n > 0$ are only considered since similar considerations can be made in all other cases ($\gamma_n > 0$, $\gamma_n < 0$, n odd, n even). In the considered case one gets

$$\overline{x} = \max\{x_t \in R : p_t(x_t, \overline{w}, \gamma) = 0, \\ \text{for some } \gamma \in \mathcal{D}_\gamma\} \tag{32}$$

and

$$\underline{x} = \min\{x_t \in R : p_t(x_t, \underline{w}, \gamma) = 0, \\ \text{for some } \gamma \in \mathcal{D}_\gamma\} \tag{33}$$

As a matter of fact equations (32) and (33) show nonlinear relations in the unknown x_t and the uncertain γ. The following considerations can be made in order to develop algorithms for the computation of $\overline{x}$ and $\underline{x}$:

1. for a given $x_t \in R$ the following facts are true:
   - if x_t is the solution of problem (32), then the set $\Gamma_t(x_t, \overline{w}, \gamma) = \{\gamma \in \mathcal{D}_\gamma : p_t(x_t, \overline{w}, \gamma) = 0\}$ is not empty;
   - if x_t is the solution of problem (33), then the set $\Gamma_t(x_t, \underline{w}, \gamma) = \{\gamma \in \mathcal{D}_\gamma : p_t(x_t, \underline{w}, \gamma) = 0\}$ is not empty;

2. let us consider the two nominal polynomials $p_t^{nom}(x_t, \overline{w}, \gamma^o)$ and $p_t^{nom}(x_t, \underline{w}, \gamma^o)$ obtained, e.g., setting $\gamma^o = \gamma^c$ and let us define $\overline{x}^o$ and $\underline{x}^o$ respectively as the maximum real root of the equation

$p_t^{nom}(x_t, \overline{w}, \gamma^o) = 0$ and the minimum real root of the equation $p_t^{nom}(x_t, \underline{w}, \gamma^o) = 0$; it is noticed that only the two intervals $[\overline{x}^o, +\infty)$ and $(-\infty, \underline{x}^o]$ have to be explored in order to find a suitable approximation of $\overline{x}$ and $\underline{x}$ respectively.

Stringing together those considerations the following two algorithms are proposed for the approximate computation of $\overline{x}$ and $\underline{x}$ respectively.

Algorithm 1. (Computation of $\overline{x}$)
1. **Set** $\alpha = \alpha_0$ and $\epsilon =$ prescribed tolerance.
2. **Compute** $r = \max\{x_t \in R : p_t^{nom}(x_t, \overline{w}) = 0, \gamma^c\}$.
3. **Set** $x_m = r$.
4. **Set** $x_M = x_m + \alpha$.
5. **If** $\exists \gamma^\diamond \in \mathcal{D}_\gamma : p_t(x_M, \overline{w}, \gamma^\diamond) = 0$ **then**
    $x_m = x_M$;
  else
    If $|x_M - x_m| < \epsilon$ **then**
      $\overline{x}_* = x_M$;
      return $\overline{x}_*$;
      stop algorithm.
    else
      $\alpha = \alpha/2$;
    end if
  end if.
8. Repeat from 4.

Algorithm 2. (Computation of $\underline{x}$)
1. **Set** $\alpha = \alpha_0$ and $\epsilon =$ prescribed tolerance.
2. **Compute** $r = \min\{x_t \in R : p_t^{nom}(x_t, \underline{w}) = 0, \gamma^c\}$.
3. **Set** $x_M = r$.
4. **Set** $x_m = x_M - \alpha$.
5. **If** $\exists \gamma^\diamond \in \mathcal{D}_\gamma : p_t(x_m, \underline{w}, \gamma^\diamond) = 0$ **then**
    $x_M = x_m$;
  else
    If $|x_M - x_m| < \epsilon$ **then**
      $\underline{x}^* = x_m$;
      return $\underline{x}^*$;
      stop algorithm.
    else
      $\alpha = \alpha/2$;
    end if
  end if.
8. Repeat from 4.

The main properties of Algorithm 1 and Algorithm 2 are highlighted by the following proposition.

***Proposition** 8.* Algorithm 1 and Algorithm 2 show the following properties:
1. Algorithm 1 and Algorithm 2 are convergent.
2. Algorithm 1 provides an upper bound $\overline{x}_*$ of $\overline{x}$ and Algorithm 2 provides an lower bound $\underline{x}^*$ of $\underline{x}$; the absolute errors of such bounds are both bounded by ϵ.
3. The check required by step 5 of Algorithm 1 and Algorithm 2 can be performed solving a linear programming problem.

Proof: see (Cerone and Regruto, 2004)

Computation of x_t^{max} and x_t^{min} — Finally, the computation of the inner signal bounds is considered. In this case one must compute

$$x_t^{max} = \max\{x_t \in \overline{X} : p_t(x_t, y_t + \Delta\eta_t, \gamma) = 0, \text{ for some } \gamma \in \mathcal{D}_\gamma\}$$

and

$$x_t^{min} = \max\{\overline{x}, \hat{x}_t^{min}\}$$

where

$$\hat{x}_t^{min} = \min\{x_t \in R : p_t(x_t, y_t - \Delta\eta_t, \gamma) = 0, \text{ for some } \gamma \in \mathcal{D}_\gamma\}$$

Since $x_t^{max} = \max\{x_t \in \overline{X} : p_t(x_t, y_t + \Delta\eta_t, \gamma) = 0, \text{ for some } \gamma \in \mathcal{D}_\gamma\} = \max\{x_t \in R : p_t(x_t, y_t + \Delta\eta_t, \gamma) = 0, \text{ for some } \gamma \in \mathcal{D}_\gamma\}$, x_t^{max} can be computed using Algorithm 1 simply substituting $p_t(x_M, \overline{w}, \gamma)$ with $p_t(x_M, y_t + \Delta\eta_t, \gamma)$. Moreover, as a matter of fact, $\hat{x}_t^{min}$ can be computed using Algorithm 2 simply substituting $p_t(x_M, \underline{w}, \gamma)$ with $p_t(x_M, y_t - \Delta\eta_t, \gamma)$.

5. A SIMULATED EXAMPLE

In this section the parameter bounding procedure outlined in (Cerone *et al.*, 2003) is applied to a numerical example exploiting the results and the algorithms developed in the present paper. The system considered here is characterized by (1), (2) and (5) with: $\gamma_1 = -5$, $\gamma_2 = -4$, $\gamma_3 = 1$, $\psi_1(u_t) = u_t$; $\psi_2(u_t) = u_t^2$; $\psi_3(u_t) = u_t^3$; $A(q^{-1}) = (1 - 1.1q^{-1} + 0.28q^{-2})$ and $B(q^{-1}) = (0.1q^{-1} + 0.08q^{-2})$. The considered nonlinear function is an odd non-invertible function. Bounded absolute output errors have been considered when simulating the collection of both steady state data, $\{\bar{u}_s, \bar{y}_s\}$, and transient sequence $\{u_t, y_t\}$. We assumed that the transient and steady-state measurement noise sequences $\{\eta_t\}$ and $\{\bar{\eta}_s\}$ are random sequences belonging to the uniform distributions $U[-\Delta\eta_t, +\Delta\eta_t]$ and $U[-\Delta\bar{\eta}_s, +\Delta\bar{\eta}_s]$ respectively. Bounds on steady-state and transient output measurement errors were supposed to have the same value, i.e., $\Delta\eta_t = \Delta\bar{\eta}_s \triangleq \Delta\eta$, and were chosen in such a way as to simulate five different values of signal to noise ratio at the output, namely 60 dB, 50 dB, 40 dB, 30 dB and 20 dB. For a given $\Delta\eta$, the length of steady-state and the transient data are $M = 50$ and $N = [100, 1000]$ respectively. From the simulated transient sequence $\{w_t, \eta_t\}$ and steady-state data $\{\bar{w}_s, \bar{\eta}_s\}$, the signal to noise ratios SNR and $\overline{SNR}$ are evaluated, respectively, through $SNR = 10 \log \left\{ \sum_{t=1}^N w_t^2 \Big/ \sum_{t=1}^N \eta_t^2 \right\}$ and $\overline{SNR} = 10 \log \left\{ \sum_{s=1}^M \bar{w}_s^2 \Big/ \sum_{s=1}^M \bar{\eta}_s^2 \right\}$.

The steady-state input sequence $\{\bar{u}_s\}$ belongs to the interval $[-10, 10]$, $u_{DC} = 7.53$ and the dynamic sequence $\{u_{td}\}$ belongs to the uniform distribution

$U[-2.45, 2.45]$. Results about the nonlinear and the linear block are reported in Table 1 and Tables 2 and 3 respectively. For low noise level ($SNR = 60$ dB) and for all N, the central estimates of both the nonlinear static block and the linear model are consistent with the true parameters. For higher noise level ($SNR \leq 40$ dB), both γ^c and θ^c give satisfactory estimates of the true parameters. As the number of observations increases (from $N = 100$ to $N = 1000$), parameter uncertainty bounds $\Delta\gamma_j = |\gamma_j^{max} - \gamma_j^{min}|/2$ and $\Delta\theta_j$ $|\theta_j^{max} - \theta_j^{min}|/2$ decreases, as expected.

6. CONCLUSIONS

In this paper the identification of SISO Wiener models has been considered when the output measurements are corrupted by unknown but bounded noise. A three stage procedure based on the inner signal estimation, outlined in a previous contribution, has been proposed. Results and algorithms for the computation of inner-signal bounds through the design of a suitable input sequence have been provided for the case of non-invertible nonlinearity. A simulated example, showing the effectiveness of the proposed approach, has been presented.

Table 1: Nonlinear block parameter central estimates (γ_j^c) and parameter uncertainty bounds ($\Delta\gamma_j$)

$\overline{SNR}$ (dB)	γ_j	True Value	γ_j^c	$\Delta\gamma_j$
58.2	γ_1	-5.000	-4.999	2.1e-3
	γ_2	-4.000	-4.000	1.8e-4
	γ_3	1.000	1.000	4.8e-5
38.2	γ_1	-5.000	-5.027	3.6e-2
	γ_2	-4.000	-3.995	8.1e-3
	γ_3	1.000	1.001	1.6e-3
28.6	γ_1	-5.000	-5.040	8.2e-2
	γ_2	-4.000	-4.003	6.2e-3
	γ_3	1.000	1.000	1.9e-3
18.4	γ_1	-5.000	-5.101	1.1e-1
	γ_2	-4.000	-4.000	1.0e-2
	γ_3	1.000	1.004	5.1e-3

REFERENCES

Bai, E.W. (2003). Frequency domain identification of Wiener models. *Automatica* **39**, 1521–1530.

Billings, S.A. (1980). Identification of nonlinear systems — a survey. *IEE Proc. Part D* **127**(6), 272–285.

Cerone, V. and D. Regruto (2004). Parameter bouds of Wiener models: input design. *DAUIN internal Report DAI0423*.

Cerone, V. M. Milanese and D. Regruto (2003). Parameters set evaluation of Wiener models from data with bounded output errors. *Proc. of 13th IFAC Symposioum on System Identification*.

Crama, P. and J. Schoukens (2001). Initial estimates of Wiener and Hammerstein systems using multisine excitation. *IEEE Trans. on Instrumentation and Measurement* **50**, 1791–1795.

Greblicki, W. (1992). Nonparametric identification of Wiener systems. *IEEE Trans. Infor. Theory* **38**, 1487–1493.

Milanese, M. Norton, J. Piet-Lahanier, H. and Walter, E. Eds.) (1996). *Bounding approaches to system identification*. Plenum Press. New York.

Wigren, T. (1993). Recursive prediction error identification using the nonlinear wiener model. *Automatica* **29**(4), 1011–1025.

Table 2: Linear system parameter central estimates (θ_j^c) and parameter uncertainty bounds ($\Delta\theta_j$) when $N = 100$.

SNR (dB)	θ_j	True Value	θ_j^c	$\Delta\theta_j$
58.2	θ_1	-1.100	-1.100	5.3e-3
	θ_2	0.280	0.280	5.1e-3
	θ_3	0.100	0.100	6.1e-4
	θ_4	0.080	0.080	5.6e-4
38.0	θ_1	-1.100	-1.106	7.9e-2
	θ_2	0.280	0.288	7.4e-2
	θ_3	0.100	0.100	8.0e-3
	θ_4	0.080	0.081	9.0e-3
28.3	θ_1	-1.100	-1.155	2.1e-1
	θ_2	0.280	0.331	2.0e-1
	θ_3	0.100	0.105	2.0e-2
	θ_4	0.080	0.074	2.9e-2
18.2	θ_1	-1.100	-1.211	3.9e-1
	θ_2	0.280	0.403	3.6e-1
	θ_3	0.100	0.099	4.2e-2
	θ_4	0.080	0.101	4.7e-2

Table 3: Linear system parameter central estimates (θ_j^c) and parameter uncertainty bounds ($\Delta\theta_j$) when $N = 1000$.

SNR (dB)	θ_j	True Value	θ_j^c	$\Delta\theta_j$
58.2	θ_1	-1.100	-1.100	1.9e-3
	θ_2	0.280	0.280	1.8e-3
	θ_3	0.100	0.100	1.9e-4
	θ_4	0.080	0.080	2.2e-4
38.4	θ_1	-1.100	-1.102	5.8e-2
	θ_2	0.280	0.282	5.4e-2
	θ_3	0.100	0.100	6.1e-3
	θ_4	0.080	0.079	5.9e-3
28.2	θ_1	-1.100	-1.106	8.9e-2
	θ_2	0.280	0.284	8.2e-2
	θ_3	0.100	0.099	8.7e-3
	θ_4	0.080	0.080	1.0e-2
18.2	θ_1	-1.100	-1.113	1.5e-1
	θ_2	0.280	0.293	1.4e-1
	θ_3	0.100	0.101	1.6e-2
	θ_4	0.080	0.078	1.7e-2